Superconducting 4-20 GHz Wideband Lumped-Element Based Hybrid for Radio Astronomy Receivers

Citation for the original published paper (version of record):
Behrens, M., Meledin, D., Belitsky, V. et al (2025). Superconducting 4-20 GHz Wideband Lumped-Element Based Hybrid for Radio Astronomy Receivers. 34th IEEE International Symposium on Space THz Technology

(article starts on next page)

Superconducting 4-20 GHz Wideband Lumped-Element Based Hybrid for Radio Astronomy Receivers

M. Behrens[1*], D. Meledin[1], V. Belitsky[1], F. Joint[1], and V. Desmaris[1],

***Abstract*—The next generation of superconducting sideband-separating radio astronomy receivers requires wide instantaneous bandwidth, high performance, and compact components. To accurately design these components with measured performance following that of the simulated performance, accurate models of these superconducting structures are required.**

In this work, we present a comparison between the simulation and measurement results of several superconducting lumped element structures intended for use in the intermediate frequency circuits in sideband-separating receivers. These structures were simulated in Keysight ADS Momentum and fabricated on 10 mil Alumina with superconducting Niobium metallization. Measurements were performed in a cryogenic probe station at 4.2 K.

***Keywords*—Superconducting microwave devices, low amplitude imbalance, low phase imbalance, lumped-element design, superconducting microwave devices, wideband hybrid couplers.**

I. Introduction

With the development of next-generation sideband-separating (2SB) and multi-pixel heterodyne radio astronomy receivers, there is a strong demand for low amplitude and phase imbalance, low loss, wide bandwidth, and physically small components [1,2]. Among the receiver circuitry, the intermediate frequency (IF) section occupies the most space due to the relatively larger wavelength resulting in physically larger structures. Therefore, miniaturizing the IF circuitry is essential for enhancing the integration density in multi-pixel systems. A crucial, and often relatively large, component of these heterodyne receiver systems is the IF hybrid, as illustrated in Fig. 1. This component provides the required power division and 90-degree phase offset between the two outputs, enabling the separation of the signal into upper and lower sidebands [3].

Both the loss and the sideband rejection ratio (SBR) contribute to the overall noise of the system, and thus minimization of both these factors is required for low noise operation of a 2SB receiver system. The SBR is dependent on the overall amplitude and phase balance of the receiver, which is a direct consequence of the hybrid performance [3, 4], highlighting the impact these components have on the system as a whole. Thus, it is important to accurately model the superconducting structures and components used in designing these hybrids in order to ensure that the required performance metrics are met.

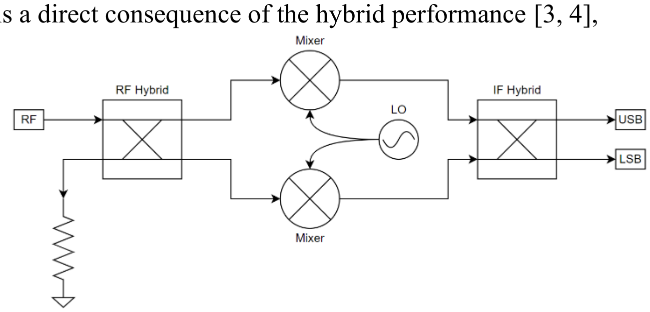

Fig. 1. Basic schematic of a 2SB heterodyne receiver

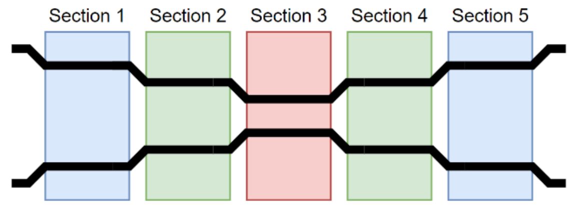

Fig.2 Schematic indicating the hybrid section numbers and the sections that have the same specifications.

The building blocks of this lumped-element based hybrid are various forms of self and mutual inductors and capacitors, the most basic of which are the series inductor and the shunt capacitor. Determining an accurate simulation model of these components will provide a stable foundation to simulate and fabricate a full lumped-element hybrid.

II. Design Methodology

The initial design of the hybrid involves determining the number of sections and corresponding coupling factors for the desired performance metrics. For a desired bandwidth of 4 to 20 GHz, a fractional bandwidth of 133%, and a passband ripple of 0.15 dB a 5-section hybrid is required with coupling factors of sections 1 and 5, 2 and 4, and 3 to be 0.09, 0.33, and 0.89 respectively [5, 6]. Fig. 2 provides clarification on the section numbering and like sections.

The coupling factor varies significantly across sections, with the outer sections, numbers 1 and 5, requiring much less coupling than the inner section, number 3. This necessitates distinct lumped-element structures to produce the desired coupling and reactive conditions.

The high coupling factor of stage 3 requires high inductive and capacitive coupling realizable through structures that demand low tolerances, emphasizing the need for accurate modelling in simulation.

Since the largest unmodelled superconducting effect is the kinetic inductance [7], most notably present in the inductors, this will be the starting point for determining the simulation model.

[1]All authors are with the Group for Advanced Receiver Development, Onsala Space Observatory, Department of Space, Earth and Environmental Sciences, Chalmers University of Technology, Gothenburg, SE-41296, Sweden. E-mail to all authors is: max.behrens@chalmers.com. *Corresponding author Max Behrens (email: max.behrens@chalmers.com).

III. EM Simulations

The simulation layout utilizes a 10 mil thick alumina substrate with two 200 nm thick Nb metallization layers and a 600 nm thick SiO_2 layer serving as a separation between the Nb layers. These structures were simulated in Keysight ADS Momentum with a perfect electrical conductor (PEC) as the metallic material.

IV. Measurement Results

A lumped inductor, as shown in Fig. 4.a, was fabricated using the same design process as for the hybrid, and measured at 4.2 K in a cryogenic probe station (Lakeshore Cryo Probe station CRX-4K, and measured with Rohde & Schwarz VNA ZVA-67). Calibration up to the probe ends was done on a standard calibration wafer (CS-5) and de-embedding of the landing pads was done using “through” and “short” measurements on the device under test (DUT). These through and short structures are displayed in Fig. 3. Fig. 5a displays a microscope image of an inductor similar to one used in the lumped hybrid with the results depicted in Fig. 5b. Sufficient correspondence between the de-embedded measurement and simulation results is achieved, with some minor deviations at the higher frequency side. This is mainly due to high frequency parasitics not considered in the de-embedding process.

V. Conclusion

We have designed, fabricated, and measured a superconducting lumped inductor with a cryogenic probe station at 4.2 K. The comparison between measurement and simulation shows sufficient correlation such that we can utilize the current model for superconducting lumped elements and further implement these structures in the design of a full lumped element hybrid.

Fig.3. Microscope image of through and a short used for de-embedding.

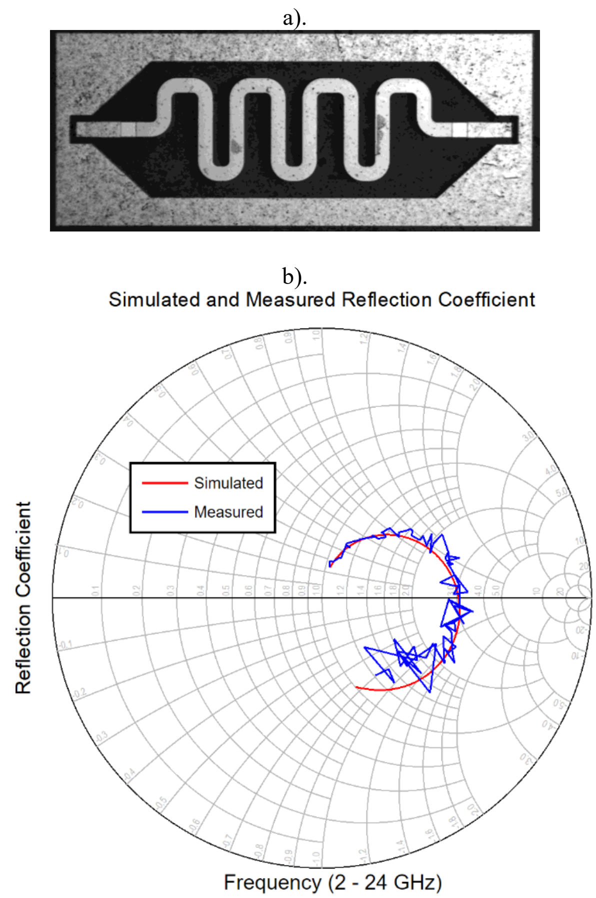

Fig.4 Nanofabricated lumped inductor, like one used in the lumped hybrid: a) microscope image of the lumped inductor; b) reflection coefficient of the measured and de-embedded (dashed blue line) inductor structure in comparison with the simulated values (red solid line).

References

[1] V. Belitsky, et al “ALMA Band 5 receiver cartridge design, performance and commissioning”, Astronomy & Astrophysics, December 13, 2017. DOI: https://doi.org/10.1051/0004-6361/201731883.

[2] Meledin, D., et al., “SEPIA345: A 345 GHz dual polarization heterodyne receiver channel for SEPIA at the APEX telescope”, Astronomy and Astrophysics, vol. 668, 2022. doi:10.1051/0004-6361/202244211.

[3] H. Rashid, D. Meledin, V. Desmaris, and V. Belitsky, “Wideband passive circuits for sideband separating receivers,” in *Proc. IEEE 29th Int. Symp. Space THz Technol.*, 2018, pp. 196–201.

[4] H. Rashid, D. Meledin, V. Desmaris, E. Sundin, and V. Belitsky. “Compact Wideband Passive and Active Component Chips for Radio Astronomy Instrumentation.” in *Proc. IEEE 29th Int. Symp. Space THz Technol.*, 2019, pp. 50-56.

[5] E. Cristal and L. Young, “Theory and tables of optimum symmetrical TEM-mode coupled-transmission-line directional couplers,” *IEEE transactions on Microwave Theory and Techniques*, vol. 13, no. 5, pp. 544–558, 1965.

[6] P. Toulios and A. Todd, “Synthesis of symmetrical TEM-mode directional couplers,” *IEEE Transactions on Microwave Theory and Techniques*, vol. 13, no. 5, pp. 536–544, 1965.

[7] V. Belitsky, C. Risacher, M. Pantaleev and V. Vassilev, 2006. Superconducting microstrip line model studies at millimetre and sub-millimetre waves. *International journal of infrared and millimeter waves*, *27*(6), pp.809-834.